Aerodynamic Design Considerations for Efficient High-Lift Supersonic Wings

David S. Miller* and Richard M. Wood*
NASA Langley Research Center, Hampton, Virginia

A previously developed technique for selecting a design space for efficient supersonic wings is reviewed. This design-space concept is expanded to include thickness and camber effects and is evaluated for cambered wings. The original design-space formulation was based on experimental upper- and lower-space normal-force characteristics for flat, uncambered delta wings; it is shown that these general characteristics hold for various thickness distributions and for various amounts of leading-edge camber. The original design-space formulation also was based on the assumption that the combination of Mach number and leading-edge sweep, which would produce an equal division of flat-wing lift between the upper and lower surface also would be the proper combination to give the best cambered-wing performance. Using the drag-due-to-lift factor as a measure of performance, cambered-wing performance is shown to significantly increase as conditions approach the design space. This correlation is demonstrated for both subcritical and supercritical flows.

Nomenclature

b = wing span
b_f = span of leading-edge flap
C_D = drag coefficient
ΔC_D = incremental change in drag coefficient from the minimum drag of a flat wing
C_L = lift coefficient
$C_{L,Crit}$ = critical lift coefficient
$C_{L,D}$ = design lift coefficient
C_{L_α} = lift-curve slope
$C_N{}^L$ = wing lower-surface normal-force coefficient
$C_N{}^U$ = wing upper-surface normal-force coefficient
C_p = pressure coefficient
M = Mach number
M_C = crossflow Mach number
M_D = design Mach number
M_N = component of Mach number normal to wing leading edge $= M\cos\Lambda(1+\sin^2\alpha\tan^2\Lambda)^{1/2}$
X, Y, Z = Cartesian coordinates
α = angle of attack
α_N = angle of attack normal to wing leading edge $= \tan^{-1}(\tan\alpha/\cos\Lambda)$
β $= \sqrt{M^2-1}$
η = fraction of wing local semispan
Λ = leading-edge-sweep angle

Introduction

FOR the past twenty years, a considerable effort has been directed toward the design of aerodynamically efficient wings for supersonic flight. The early efforts were directed at transport-type aircraft. For these small-disturbance producing aircraft, linearized-theory zero-thrust attached-flow optimization procedures[1,2] successfully produced efficient twisted- and cambered-wing designs. These wings were characterized by low-wing loadings which made it possible to produce wing designs within the limits of subcritical flow; thus, it was believed that these designs would remain well within the applicable range of linearized theory. However, many of the subcritical designs did not experimentally achieve the theoretically predicted reductions in drag-due-to-lift.[3] More recently, studies have addressed the high-lift ($C_L \approx 0.4$) wing design problem[4-7] which, according to Brown et al.'s criterion,[8] requires supercritical flow on the wing upper-surface. Although the target pressure distributions were achieved, and the drag due to lift was significantly reduced from the flat-wing value, the resulting drag reduction was only about 50% of the linearized theory predicted minimum value. In general, both the subcritical and supercritical wing designs involved determining the wing warp (twist and camber) required to produce a given lift on a given planform at a specified Mach number. The selection of the wing planform, in general, was not made to produce the most efficient supersonic aerodynamic performance but was a compromise between subsonic, transonic, and structural considerations. In fact, except for linear theory guides, there seems to be no experimentally verified criterion for selecting a wing planform based on supersonic performance—and the linearized theory guidelines would indeed not be applicable for high-lift designs.

In a recent study[9] of the supersonic aerodynamics of delta wings, a design space was identified that coupled the parameters of Mach number, leading-edge sweep, angle of attack, and lift coefficient. The design space was based on maintaining a specific relationship between upper- and lower-surface flow conditions; wing performance was not correlated. It is the purpose of this paper to investigate this idea further by correlating wing performance with the design-space concept of Ref. 9 for several subcritical and super-critical wing designs.

The design-space concept set forth in Ref. 9 is discussed and expanded to include the effects of thickness and camber. From experimental values of lift-curve slope, using the design-space criterion, nominal design conditions are selected. It is shown that for these nominal conditions a moderately high-lift design ($C_L \approx 0.2$) would fall in the category of subcritical flows and a high-lift ($C_L \approx 0.4$) design would require highly nonlinear supercritical flow conditions on the leeward side of the wing. Using drag due to lift as a measure of performance, the experimental data from several subcritical and supercritical wing design studies are evaluated and the results are correlated with the design-space concept.

Presented as Paper 85-4076 at the AIAA 3rd Applied Aerodynamics Conference, Colorado Springs, CO., Oct. 14-16, 1985; received Nov. 3, 1985, revision received July 3, 1986.

*Aerospace Technologist, Fundamental Aerodynamics Branch, High-Speed Aerodynamics Division. Member AIAA.

Design-Space Concept

Supersonic design spaces for lift coefficient values of 0.2 and 0.4 are shown in Fig. 1. The design space is presented in terms of conditions normal to the leading edge, specifically, normal Mach number M_N and normal angle of attack α_N. These parameters were found to be the most convenient because they couple the effects of Mach number, leading-edge sweep, and angle of attack, thereby reducing a complex three-dimensional representation to a much simpler two-dimensional representation.

As indicated at the top of Fig. 1, the design-space criterion requires that the upper-surface normal force be equal to, or greater than, the lower-surface normal force. This criterion was presented in Ref. 9 as a hypothesis based on the authors' experiences in performing supersonic wing designs using both linearized-theory optimization codes[10] and nonlinear wing analysis codes.[11] When using unconstrained linearized-theory optimization methodology, the design-space criterion is satisfied automatically because the upper-surface pressure is equal and opposite to the lower-surface pressure and thus the upper- and lower-surface normal forces are exactly equal. If real flow constraints, such as the vacuum limit, are placed on the allowable upper-surface pressure, at some design conditions the upper-surface normal force is limited. For these conditions the constrained optimization procedure produces a wing design for which the design-space criterion is violated, and theoretically the constrained wing design has lower aerodynamic performance than the unconstrained wing design.[12] When using nonlinear aerodynamic methodology, no direct optimization procedure is available for supersonic wing design; therefore, the primary design method was to select wing geometry, which would distribute the upper-surface loading so that strong crossflow shocks and leading-edge expansion pressure peaks would be avoided.[13] Such upper-surface load distributions were achieved when the upper-surface loading was of sufficient magnitude to equal or exceed the lower-surface loading. Based on these wing-design experiences, the design-space was hypothesized.

As shown in Fig. 1, the upper boundary of the design space represents conditions at which increases in either normal Mach number or normal angle of attack will result, in conditions which violate the design-space criterion. The design space has an arbitrary lower boundary of $M = 1.2$ imposed by the limits of the conical flow assumptions used in constructing the design space. Vertical constant leading-edge-sweep lines of $\Lambda = 55$ and 75 deg are shown, respectively, on the left and right sides of the design space for reference purposes.

The design spaces of Fig. 1 indicate that a reduction in the lift coefficient from 0.4 to 0.2 expands the design space to higher Mach numbers and shifts it into a region of lower M_N and α_N. The expansion of the $C_L = 0.2$ to higher Mach numbers results from a softening of the vacuum-limit effect. The apparent reduction in the size of the design space in reducing C_L from 0.4 to 0.2 is strictly graphical due to the nonlinear relationship between the defining parameters.

The upper- and lower-surface normal-force characteristics, which were used in constructing the design spaces for Fig. 1, are shown in Fig. 2. These data represent a Mach number range from 1.5 to 3.5 and a range of leading-edge-sweep angles from 58 to 85 deg. The individual upper- and lower-surface normal-force coefficients were obtained by integrating experimentally measured spanwise pressure distributions. As shown in Fig. 2, when the upper-surface normal force ($C_N{}^U$) is plotted as a function of the parameter $\alpha_N \beta \cot\Lambda$, the data reduces to a family of constant Mach number curves. The large effect that increasing Mach number has on limiting the upper-surface normal force is clearly shown; for example, an increase in Mach number from 1.5 to 2.0 reduces the upper-surface normal force by 50%. In a similar manner, when the lower-surface normal force is plotted against normal angle of attack (α_N), the data reduces to a family of curves which vary with leading-edge-sweep angle and these curves are essentially independent of Mach number. In summary, the data in Fig. 2 show that the upper-surface normal force is primarily a function of Mach number and that the lower surface is characterized primarily by leading-edge-sweep effects.

If this design-space concept is going to be of practical use for selecting the proper combination of M, Λ, and C_L, it must be essentially independent of wing planform, airfoil thickness, and wing camber effects. In order to investigate planform, thickness, and camber effects, is necessary to have upper- and lower-surface pressure distributions complete enough to determine the upper- and lower-surface contributions to normal force. If the wing geometry is conical, the flow can be assumed conical, and a single spanwise pressure distribution is enough to determine these normal-force contributions. A wing planform investigation, which would include other than straight leading-edge wings (straight leading-edge delta wings of various sweep angles were included in the data of Fig. 2 and 3), would require the analysis of nonconical flows. In order to conduct the analysis, a very detailed set of pressures would be required over both surfaces of the complete wing planform to determine the upper- and lower-surface normal-force contributions. Unfortunately, such a set of data has not been found for a parametric set of non-delta wing planforms. Thus, using existing data, it is not possible to investigate planform effects by analyzing upper and lower-surface normal-force

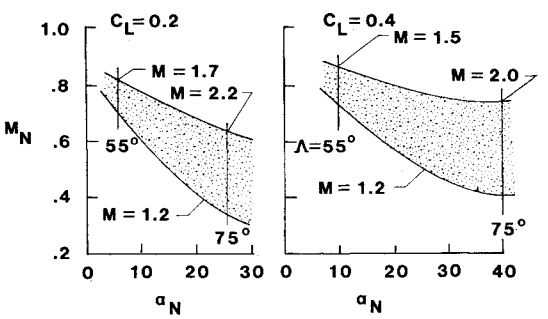

Fig. 1 Supersonic high-lift design space.

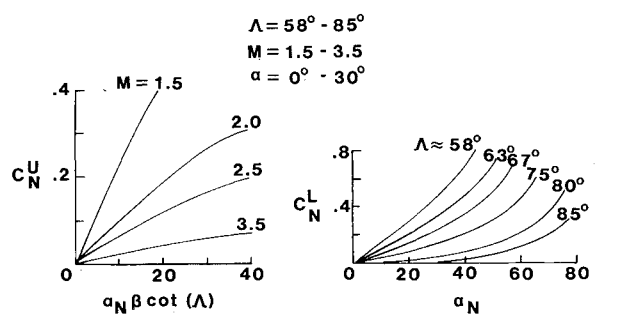

Fig. 2 Upper- and lower-surface normal forces on flat delta wings.

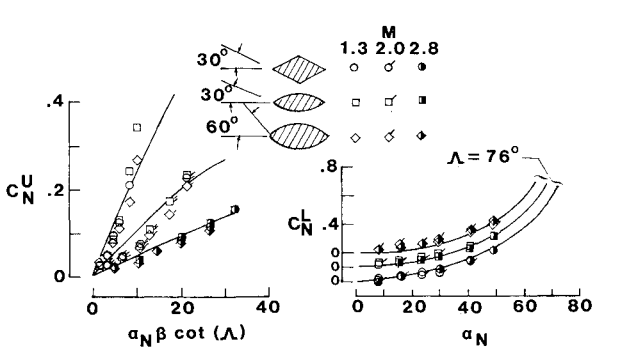

Fig. 3 Effect of thickness on character of upper- and lower-surface normal forces.

contributions; however, non-delta wing planforms are examined in subsequent discussions relating drag characteristics to the wing design space. Surface pressure data are available to construct upper- and lower-surface normal-force coefficients to examine thickness and camber effects for conical geometries, and these results are shown in Fig. 3 and 4.

In Fig. 3, upper- and lower-surface normal-force results are shown for conical delta wings of different thicknesses. The thick-wing normal-force results were constructed from spanwise pressure distributions measured at Mach numbers of 1.3, 2.0, and 2.8 on three aspect ratio 1 delta wing models differing only in thickness.[14] As shown by the sketches in the figure, the three different thicknesses correspond to a diamond cross section with a 30 deg leading-edge half angle and two biconvex circular-arc cross sections with leading-edge half angles of 30 and 60 deg. Although these conical-wing geometries do not represent typical airfoil shapes over their entire length, they do typify a practical range of wing leading-edge shapes and thickness angles. For this reason, the thickness effects observed in Fig. 3 are more or less leading-edge thickness effects and could be altered by further examining nonconical geometries. Nevertheless, in the left portion of Fig. 3, it is observed that the upper-surface normal-force data tend to separate into three groups according to Mach number and the thick-wing data agree very well with the flat-wing data (solid line in Fig. 3) of Fig. 2. In the right portion of Fig. 3, the lower-surface normal-force data follow almost exactly the flat-wing data corresponding to $\Lambda = 76$ deg; unfortunately, no data were available to examine thickness effects at other leading-edge-sweep angles. For the data examined in Fig. 3, the normal-force characteristics of the delta wings were observed to be essentially independent of wing thickness.

In Fig. 4, upper- and lower-surface normal-force results, constructed from the conical-wing pressure data of Ref. 15, are presented at a single Mach number of 1.9 for six cambered wings all having a leading-edge flap deflection angle of 15 deg. As indicated in the figure, the six wings consisted of two different flap sizes ($b_f/b = 0.10$ and 0.20) for each of the three different wing leading-edge-sweep angles (58.25, 67.5, and 75 deg). The upper-surface normal-force coefficient data tend to collapse about the $M = 1.9$ flat-wing results (solid line) and show no perceptable effects of leading-edge sweep, flap size, or flap deflection. The lower-surface normal-force coefficient data tend to separate into three groups corresponding to the different leading-edge-sweep values, and these three groups of data have the same characteristics as the flat-wing results (solid lines). Unfortunately, this cambered-wing data were obtained only at a single Mach number of 1.9; consequently, the independence of the lower-surface normal force on Mach number cannot be completely established for these series of cambered wings.

The collective results of Figs. 2, 3, and 4 indicate that the characteristics of the upper- and lower-surface normal forces of delta wings are not strong functions of thickness or camber; thus, the design spaces derived for flat, uncambered, delta wings will hopefully serve as guidelines for the design of twisted and cambered wings having practical thicknesses.

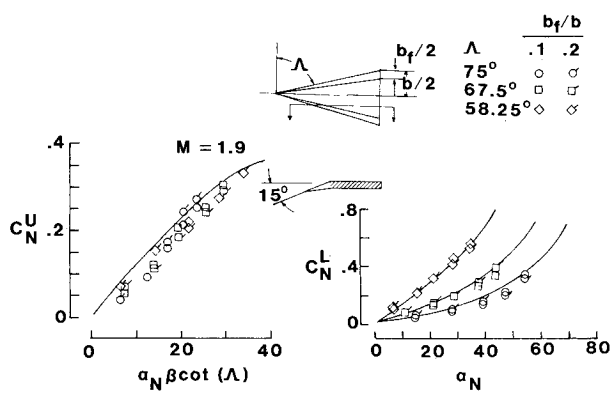

Fig. 4 Effect of camber on character of upper- and lower-surface normal forces.

Nominal Design Conditions

For both subcritical and supercritical flow conditions, nominal design conditions of the leading-edge-sweep angle, Mach number, and lift coefficient are determined. The leading-edge-sweep angle and the Mach number are determined by examining the experimental lift-curve slope and its relationship with the design space of Fig. 1. Once nominal values of the leading-edge-sweep angle and Mach number are determined, Brown et al.'s criterion[8] is used to select nominal values of lift coefficient, which correspond to either subcritical or supercritical flow conditions on the leeside of the wing. The procedure for selecting the subcritical and supercritical nominal design conditions can be illustrated with the aid of Figs. 5–7.

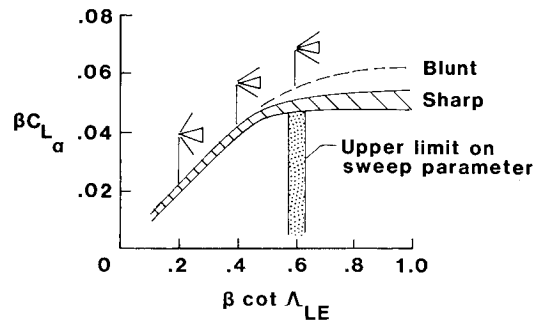

Fig. 5 Selection of leading-edge-sweep parameter using lift-curve slope.

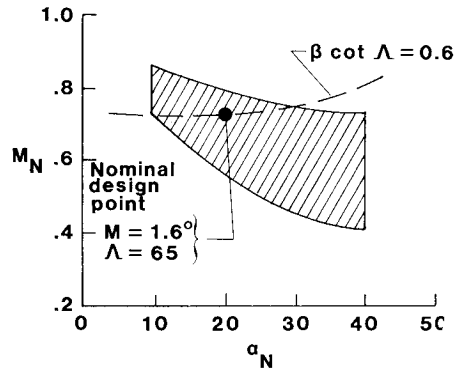

Fig. 6 Selection of nominal design point for $C_L = 0.4$.

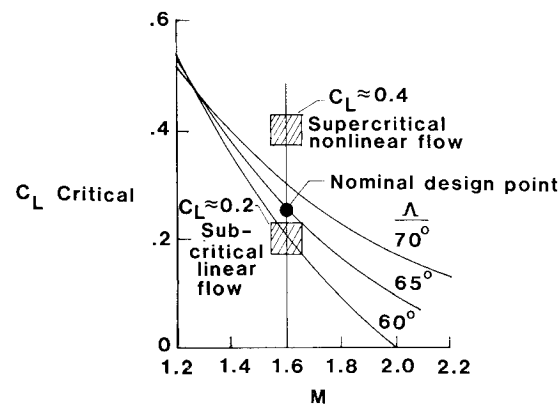

Fig. 7 Brown et al.'s[8] critical C_L criterion.

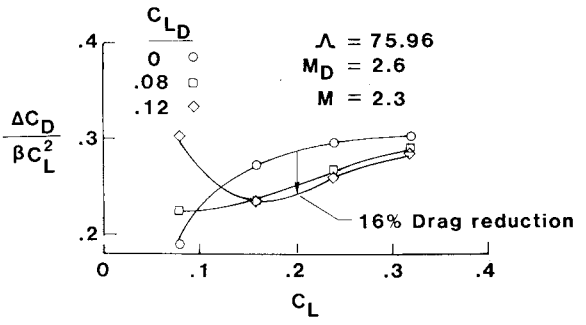

Fig. 8 Evaluation of subcritical cambered-wing performance at $C_L = 0.2$.

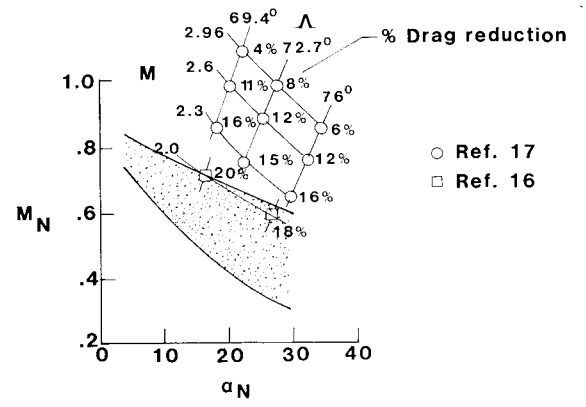

Fig. 9 Subcritical cambered-wing performance related to $C_L = 0.2$ design space.

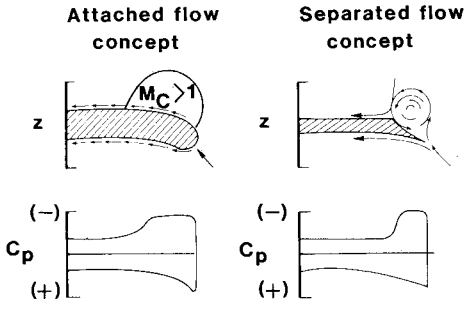

Fig. 10 High-lift design approaches for nonlinear flows.

The experimental lift-curve slope for uncambered delta wings is shown in Fig. 5 as a function of the leading-edge-sweep parameter, β cotΛ. The lift-curve slope can be used as a measure of flat-wing efficiency where the smallest drag-due-to-lift factor corresponds to the largest value of lift-curve slope. As shown in the figure, the lift-curve slope increases with leading-edge-sweep parameter until it reaches a value of $\beta C_{L_\alpha} \approx 0.05$ at β cot$\Lambda = 0.6$ for sharp leading edges. Slightly higher values can be used for blunt leading edges. A value of β cot$\Lambda = 0.6$ was selected for our nominal conditions because larger values do not improve the drag-due-to-lift characteristics of flat delta wings.

Using a value of $\beta C_{L_\alpha} = 0.05$ and values of M and Λ, which satisfy β cot$\Lambda = 0.6$, a curve corresponding to $C_L = 0.4$ was constructed in terms of the normal flow parameters, M_N and α_N. This curve is shown in Fig. 6, along with the $C_L = 0.4$ design space of Fig. 1. It was found that the β cot$\Lambda = 0.6$ curve corresponds to a wide range of M, Λ, and α conditions, which lie within the design space. A nominal design point of $M = 1.6$ and $\Lambda = 65$ deg was selected because this point is centrally

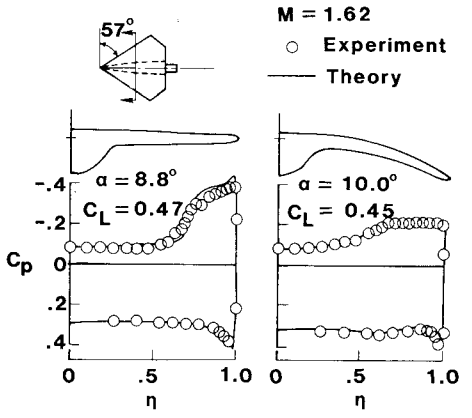

Fig. 11 Evaluation of conical-wing pressures.

located both on the β cot$\Lambda = 0.6$ curve and in the design space well away from the design-space boundaries.

This nominal design condition was analyzed to determine the nature of the flow. This analysis is shown in Fig. 7 where $C_{L,\text{Crit}}$ is plotted against M for leading-edge-sweep angles of 60, 65, and 70 deg. According to Brown et al.'s criterion,[8] for $M = 1.6$ and $\Lambda = 65$ deg supercritical flow will be required to produce lift coefficients above $C_{L,Crit} = 0.26$ and lift coefficients below this value can be produced with subcritical flows. For the subsequent evaluation of the design-space concept, the lift coefficient value of 0.2 was selected for subcritical leeside flows, and the lift coefficient value of 0.4 was selected for supercritical leeside flows.

Subcritical Camber Design Evaluation

For the reasons discussed in the previous section, it was decided to perform the design-space evaluation for subcritical cambers at a lift coefficient of 0.2 and the nominal conditions of $M = 1.6$ and $\Lambda = 65$ deg. The literature was reviewed for experimental data on cambered wings, which had been designed for these nominal conditions using linear-theory optimization techniques. Since the purpose is to analyze lifting efficiency, the experimental drag-due-to-lift factor was chosen as the figure of merit. Thus, the experimental data had to include flat uncambered wing data as well as the cambered-wing data. A review of the literature did not uncover any information on camber designs specifically at $C_L = 0.2$ for the nominal conditions; however, several studies had been conducted at slightly lower design lift coefficients (0.12 to 0.16) and at Mach numbers and leading-edge-sweep angles in the vicinity of the nominal values. The slightly lower design C_L was found to provide excellent information for $C_L = 0.2$ evaluation purposes because linear-theory techniques tend to overcamber, i.e., a camber designed for $C_L = 0.16$ experimentally will yield a better drag-due-to-lift factor at a slightly higher lift coefficient. The data from several studies were analyzed and all yielded similar drag-due-to-lift characteristics; thus, results are presented for only the studies of Refs. 16 and 17.

In the study of Ref. 16, a total of five arrow-wing models were tested at a Mach number of 2.05. Three of the wings, having a leading-edge-sweep angle of 70 deg and an aspect ratio of 2.24, were designed to produce a minimum drag at lift coefficients of 0, 0.08, and 0.16. A fourth and fifth wing, having 75 deg swept leading edge and an aspect ratio of 1.65, were designed for lift coefficients of 0 and 0.16. The airfoil thickness distribution for all wings was a 3% circular-arc section in the streamwise direction, which was added symmetrically to the mean camber surface.

In the study of Ref. 17, a total of nine modified arrow wing models were tested at Mach numbers of 2.3, 2.6, and 2.96. The wings had leading-edge-sweep angles of 69.44, 72.65, and 75.96 deg, which correspond to values of the design-Mach-number-sweep-angle parameter (β cotΛ) of 0.6, 0.75, and 0.9,

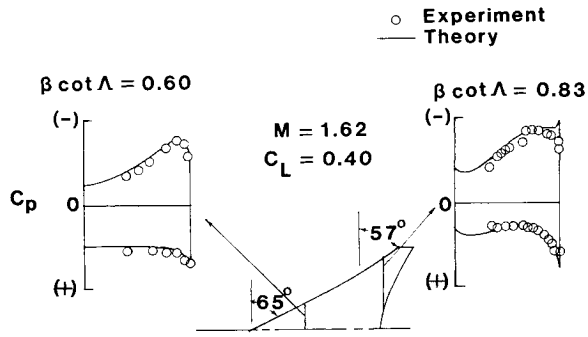

Fig. 12 Evaluation of three-dimensional wing pressures.

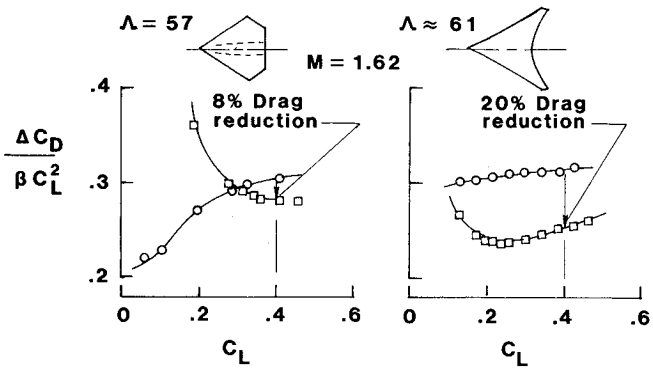

Fig. 13 Evaluation of supercritical cambered-wing performance at $C_L = 0.4$.

respectively. For each sweep angle, there were three camber surfaces having design lift coefficients of 0, 0.08, and 0.12 at a design Mach number of 2.6.

Because the drag-due-to-lift characteristics of all the subcritical wing camber designs were similar, a typical data set from Ref. 17 is shown in Fig. 8 to illustrate the performance evaluation procedure. For the $\Lambda = 76$ deg planform, the drag-due-to-lift parameter is plotted as a function of lift coefficient for each of the three wing cambers ($C_{L,D} =$ 0.08, and 0.12). This figure clearly illustrates that linear theory overcambers; the $C_{L,D} = 0.08$ camber is not effective in reducing the flat-wing drag due to lift at lift coefficients below $C_L = 0.10$ and the $C_{L,D} = 0.12$ camber produces a minimum drag due to lift at $C_L = 0.16$. The two cambered-wing curves cross at $C_L = 0.16$ and are increasing and running parallel at $C_L = 0.2$ where the $C_{L,D} = 0.12$ camber is producing slightly less drag due to lift than the $C_{L,D} = 0.08$ camber. It also should be noted that if these results are extrapolated out to a supercritical condition of $C_L = 0.4$, little or no reduction in the flat-wing drag due to lift would be produced by either of the subcritical cambered wing designs. For this study, the cambered-wing performance at $C_L = 0.2$ is computed as a percent drag reduction with respect to the flat-wing drag; for the example in Fig. 8, the maximum cambered-wing performance corresponds to a 16% drag reduction for the $C_{L,D} = 0.12$ camber at a lift coefficient of 0.2.

The relationship between the subcritical cambered-wing performance and the $C_L = 0.2$ design space is shown in Fig. 9. Performance was computed at nine different Λ-M combinations for data from Ref. 17 and at two combinations from Ref. 16. It is clearly shown that the data closest to the design space have the best performance; e.g., in the matrix of data of Ref. 17, the data point furthest from the design space only has a 4% drag reduction, whereas the data point closest to the design space has a 16% drag reduction. Both the data points of Ref. 16 lie near the upper boundary of the design space, and these points have drag reductions as high as 20%. Although none of the data examined were located well within the design space, it might be concluded from the information of Fig. 9 that drag reductions of 25-30% could be expected for subcritical cambered wings designed to operate within the design space. Also, all of the data examined supported the design-space concept, i.e., performance improved as operating conditions approached the design space.

Supercritical Camber Design Evaluation

A lift coefficient of 0.4 was selected for the supercritical camber evaluation. These high levels of lift require flow conditions that lie outside the linear theory regime; and, as shown in Figure 10, both attached and separated nonlinear flows are explored for designing efficient high-lift supersonic wings. Figure 10 shows a sketch of the spanwise flow and spanwise pressure distribution for two quite different nonlinear flow concepts under investigation. The object of the attached flow concept is to achieve efficient high levels of lift through a controlled supercritical expansion around a rounded leading edge; the objective of the separated flow concept is to achieve efficient high lift through a controlled leading-edge vortex emanating from a sharp leading edge. Note that the pressure distributions are very similar for these very different types of flow.

For supersonic speeds, the separated flow wing design concept has undergone some significant developments over the past several years, e.g., types of separated flows have been classified for delta wings,[14] and considerable progress has been made in the development of calculation techniques.[19-23] However, no supersonic, separated-flow wing designs have yet been experimentally tested and thus no supersonic performance data is available for evaluation purposes. On the other hand, the attached supercritical nonlinear flow wing design concept has been applied and two sets of experimental data[4-7] are available for evaluating the design-space concept.

The first data set resulted from the design, analysis, and testing of conical wing[4,5] and the second data set resulted from a similar study of a more practical fully three-dimensional wing.[6,7] A full potential flow code[11] capable of accurately analyzing highly nonlinear supersonic flows with embedded crossflow shocks was used to perform the designs by iteration; no direct design method exists. Both surface pressures and longitudinal forces and moments were measured in the experimental tests.

The conical wing data set was obtained on a cambered wing and a comparison flat wing. Both wings had 57 deg of leading-edge sweep and the same thickness distribution. The cambered wing was designed at a Mach number of 1.62 for a pressure distribution which would produce a lift coefficient of approximately 0.45 at 10 deg angle of attack and which would have no leading-edge expansion pressure peak and no recompression crossflow shock. The cambered-wing spanwise pressure distribution in Fig. 11 clearly shows that the theoretical pressure distribution was achieved experimentally. For approximately the same lift, the flat-wing pressure distribution exhibits a much larger leading-edge expansion followed by a strong recompression. These flat-wing pressure results are obviously less desirable than the cambered-wing results, and the cambered wing did produce less drag than the flat wing. However, the pressure distributions of both wings indicate that the lower surface is producing considerably more lift than the upper surface. Because this observation is in conflict with the design-space criterion, the design conditions probably lie outside the design space and the performance benefits should be small; these facts will be substantiated in the subsequent discussion.

The second data set was obtained on a more practical fully three-dimensional cambered wing. Again, the design Mach number was 1.62; however, the wing planform had continuously varying leading-edge sweep, which ranged from 65 deg inboard to 57 deg outboard. On the average, the three-dimensional wing had 61 deg of leading-edge sweep or 4 deg more sweep than the conical wing planform.

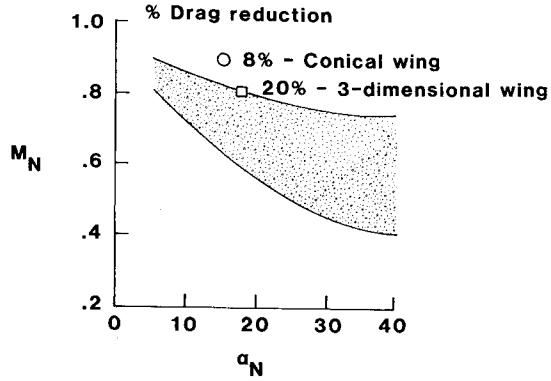

Fig. 14 Supercritical cambered-wing performance related to $C_L = 0.4$ design space.

In Fig. 12, at the design lift coefficient of 0.4, experimental and theoretical spanwise pressure distributions are shown for the two extreme leading-edge-sweep conditions. At the largest sweep condition, the desired shockless recompression was achieved experimentally, and at the condition of least sweep, a small shock can be observed in the experimental data. In general, the theoretical pressure distributions were achieved experimentally. In contrast to the conical wing pressure data, the pressure data for the three-dimensional wing indicate that the lift is distributed approximately equally between the upper and lower surfaces; thus, the three-dimensional wing conditions more closely correspond to the the design space criterion, and the performance benefits should be better than those from the conical wing study.

In Fig. 13 the experimental drag-due-to-lift parameter is plotted as a function of lift coefficient for cambered and uncambered versions of the conical and three-dimensional wings. Because an uncambered version of the three-dimensional wing was not constructed and tested, the drag-due-to-lift parameter shown for this wing is taken from the lift-curve slope of the cambered wing. This method of determing the drag due to lift for flat wings can be very inaccurate at low-lift conditions; however, it is an adequate representation for high-lift conditions. The performance evaluation was conducted at a lift coefficient of 0.4; the conical wing data showed an 8% drag reduction and the three-dimensional wing data showed a 20% drag reduction.

The relationship between the supercritical cambered-wing performance and the $C_L = 0.4$ design space is shown in Fig. 14. Only one Λ-M combination is shown for the conical wing and one combination for the three-dimensional wing. Again, it is clearly shown that the data point closest to the design space has the best performance; i.e., the three-dimensional wing result, which lies on the design-space boundary, produced a 20% drag reduction as compared to the conical wing result, which is considerably above the design-space upper boundary and produced only an 8% drag reduction.

Summary

A previously developed technique for efficient supersonic wings has been reviewed, expanded to include thickness and camber, and evaluated for high-lift conditions. The original design-space formulation was based on experimental upper-surface and lower-surface normal-force characteristics for flat, uncambered delta wings; it was shown that these general characteristics hold for various thickness distributions and for various amounts of leading-edge camber. The original design-space formulation also was based on the assumption that the proper combination of Mach number and leading-edge sweep, which would produce an equal division of flat-wing lift between the upper and lower surfaces, would also be the proper combination to give the best cambered-wing performance; in terms of drag due to lift, cambered-wing high-lift performance was shown to increase significantly as conditions approached the design space; this relationship was shown to hold for both subcritical and supercritical flow conditions.

References

[1]Carlson, H.W. and Middleton, W.D., "A Numerical Method for the Design of Camber Surfaces of Supersonic Wings with Arbitrary Planforms," NASA TN D-2341, 1964.

[2]Carlson, H.W. and Miller, D.S., "Numerical Methods for the Design and Analysis of Wings at Supersonic Speeds," NASA TN D-7713, 1974.

[3]Carlson, H.W. and Miller, D.S. "The Influence of Leading-Edge Thrust on Twisted and Cambered Wing Design for Supersonic Cruise", AIAA Paper 81-1656, 1981.

[4]Mason, W.H. and Miller, D.S. "Controlled Supercritical Crossflow on Supersonic Wings—An Experimental Validation," AIAA Paper 80-1421, July 1980.

[5]Miller, D.S., Landrum, E.J., Townsend, J.C., and Mason, W.H., "Pressure and Force Data for a Flat Wing and a Warped Conical Wing Having a Shockless Recompression at Mach 1.62," NASA TP-1759, April 1981.

[6]Mason, W.H., Miller, D.S., Pittman, J.L., and Siclari, M.J., "A Supersonic Maneuver Wing Designed for Nonlinear Attached Flow," AIAA Paper 83-0425, 1983.

[7]Pittman, J.L., Miller, D.S., and Mason, W.H. "Supersonic, Nonlinear, Attached-Flow Wing Design for High Lift With Experimental Validation," NASA TP-2336, Aug. 1984.

[8]Brown, C., McLean, F., and Klunker, E. "Theoretical and Experimental Studies of Cambered and Twised Wings Optimized for Flight at Supersonic Speeds," *Proceedings of the 2nd International Congress of Aeronautical Sciences, Advance in Aeronautical Science,* Vol. 3, edited by T. von Karman, et al., Pergamon Press, Oxford, 1962.

[9]Wood, R.M. and Miller, D.S., "Fundamental Aerodynamic Characteristics of Delta Wings with Leading-Edge Vortex Flows," *Journal of Aircraft*, Vol. 22, June 1985, p. 479.

[10]Middleton, W.D., Lundry, J.L., and Coleman, R.G., "A System for Aerodynmaic Design and Analysis of Supersonic Aircraft. Part 2—User's Manual," NASA CR-3352, 1980.

[11]Siclari, M.J., "The NCOREL Program for 3D Nonlinear Supersonic Potential Flow Computations," NASA CR-3694, 1983.

[12]Miller, D.S. and Middleton, W.D., "An Integrated System for the Aerodynamic Design and Analysis of Supersonic Aircraft," NASA SP-247, March 1975.

[13]Miller, D.S., "Supersonic Wing Design Concepts Employing Nonlinear Flows," Paper presented at the 14th Congress of the International Council of the Aeronautical Sciences, Toulouse, France, ICAS Paper 84-1.8.1, Sept 21-23, 1984.

[14]Britton, J.W. "Pressure Measurements at Supersonic Speeds on Three Uncambered Conical Wings of Unit Aspect Ratio," British Aeronautical Research Council, CP-641, 1963.

[15]Michael, W.H., Jr., "Flow Studies on Drooped-Leading-Edge Delta Wings at Supersonic Speed," NACA TN-3614, Jan. 1956.

[16]Carlson, H.W., "Aerodynamic Characteristics at Mach Number 2.05 of a Series of Highly Swept Arrow Wings Employing Various Degrees of Twist and Camber," NASA TM X-332, Oct. 1960.

[17]Mack, R.J., "Effects of Leading-Edge Sweep Angle and Design Lift Coefficient on Performance of a Modified Arrow Wing at a Design Mach Number of 2.6," NASA TN D-7753, Dec. 1974.

[18]Miller, D.S. and Wood, R.M., "Lee-Side Flows Over Delta Wings at Supersonic Speeds," NASA TP-2430, June 1985.

[19]Rizzi, A., Eriksson, L.E., Schmidt, M., and Hitzel, S., "Numerical Solutions of the Euler Equations Simulating Vortex Flows Around Wings," AGARD-CP-342, 1983.

[20]Rizetta, D.P. and Shang, J.S., "Numerical Simulation of Leading-Edge Vortex Flows," AIAA Paper 84-1544, June 1984.

[21]Raj, P. and Sikora, J.S., "Free-Vortex Flows: Recent Encounters with an Euler Code," AIAA Paper 84-0135, Jan. 1984.

[22]Newsome, R.W., "A Comparison of Euler and Navier-Stokes Solutions for Supersonic Flow Over a Conical Delta Wing," AIAA Paper 85-0111, Jan. 1985.

[23]Murman, E.M., Rizzi, A., and Powell, K., "High Resolution Solutions of the Euler Equations for Vortex Flows," *Progress & Supercomputing in Computational Fluid Dynamics*, Birkhauser, Boston, MA, Inc. 1985.

[24]Siclari, M.J., "The NCOREL Computer Program for 3D Nonlinear Supersonic Potential Flow Computations," NASA CR-3694, Aug. 1983.